

MEASUREMENT OF THIN CLOUD OPTICAL PROPERTIES USING A COMBINED MIE-RAMAN LIDAR

Yonghua Wu, Shuki Chaw, Barry Gross, Yu Zhao, Fred Moshary, Sam Ahmed

NOAA-CREST, The City College of New York, New York, NY 10031, E-mail: yhwu@ccny.cuny.edu

ABSTRACT

A multiple-wavelength Mie-Raman lidar has been developed for aerosol, cloud and water vapor measurement over the Metropolitan area of New York. In this presentation, extinction, backscatter and lidar ratios profiles are obtained under daylight conditions for both aerosol and low water phase clouds. To validate the profiles, the optical depths of the low altitude clouds are derived using two independent methods. In particular, excellent agreement for the optical depth measurements between the regression technique using elastic backscatter profiles below and above the cloud and the integrated extinction from the N₂-Raman returns is obtained. Furthermore, it is shown that to obtain accurate optical depths, a modified regression approach accounting for aerosol backscatter below cloud base is needed. Finally, the usefulness of the raman profiles for determining the effective water droplet size is presented.

1. MIE-RAMAN LIDAR DESCRIPTION

A multiple-wavelength Mie-Raman lidar has been built for aerosol and cloud measurements at CCNY campus (40.819°N/73.949°W), New York. The transmitter is a Nd:YAG laser (Quanta-Ray PRO-230, 30Hz) operating at 355nm, 532nm and 1064nm. A Newtonian telescope with a 1.5-mrad field of view and receiver diameter 50.4-cm is used to collect the backscatter returns. Elastic returns (Mie and Rayleigh) at 355-532-1064-nm along with N₂-Raman returns at 387 nm are received simultaneously. The schematic layout is shown in figure 1.

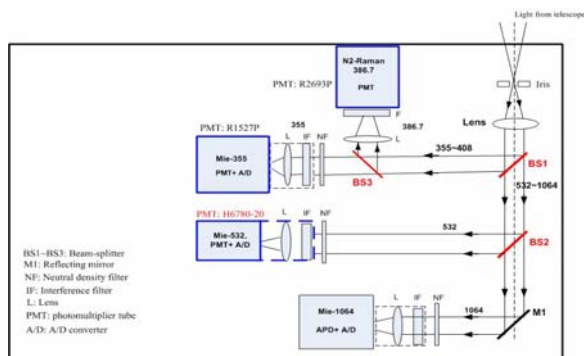


Fig. 1 Raman Lidar configuration

Three photomultiplier tubes (Hamamatsu PMT) are used for the UV-Visible returns while a Si-APD detector is used for 1064-nm channel. A narrow-band interference filter (Barr Assoc., BW=0.3-nm) is used to suppress the skylight background noise and act as an interference filter for the N₂-Raman channel. The filter is designed to effectively eliminate interference from the elastic returns. The elimination of cross-talk was confirmed by the absence of a raman signal due to low clouds. The detector outputs are acquired by Licel transient recorders, which combine A/D and photon counting techniques (16-bit 40 MHz A/D and 250 MHz photon counter). In our standard processing mode, Lidar signal profiles are recorded by 1-min average (1800 laser shots) and 3.75 m range resolution. For our system, the overlap function is close to unity to within a few hundred meters even though it is coaxial.

2. MEASUREMENT THEORY

Aerosol and cloud retrievals by Mie-Raman lidar are well described in the literatures [1-3]. Briefly, aerosol extinction can be directly derived from N₂-Raman signals provided we account for the molecular extinction and backscatter (i.e. number density). To extrapolate the extinction from the raman channel at 387 nm to the elastic channel at 355 nm, an angstrom exponent is needed and taken to be 1.0 for aerosol and 0.0 for cloud. While the derived aerosol extinction could then be fed into the single scatter lidar equation for the elastic channel, it is more convenient to obtain the backscatter ratio $R = (\beta_a + \beta_m) / \beta_m$ by taking the ratio between the elastic signal and the Raman signal. From these two independent measurements, the extinction-to-backscatter ratio, or lidar ratio, can be calculated.

In these calculations, the molecular extinction and number density data are calculated using radiosonde data at Brookhaven site (OKX Upton), Southeast about 57 miles far from lidar site. Uncertainties of aerosol extinction and backscatter are mainly caused by the signal noises compared to the weak Raman returns in the daytime.

To assess the accuracy and consistency of these measurements, we first calculate the optical depth of low altitude clouds which are sufficiently thin so that the lidar may penetrate above the cloud with

sufficient SNR. In making this calculation, the optical depth of the cloud can obviously be obtained by integrating the extinction profiles through the cloud. However, the optical depth of a thin cloud can also be derived by regressing the theoretical molecular returns to the measured elastic returns below and above cloud, respectively [4].

The method given above is applicable only when no aerosol exists above or below cloud base and it therefore primarily used for high cirrus. However, in our case, significant aerosol will occur so the formulation must be slightly modified. To this end, we consider the correction of aerosol scattering ratio (ratio of total backscatter to only molecular backscatter) for the low clouds. Below cloud (range $z_1 \sim z_2$) and above cloud ($z_3 \sim z_4$), slopes are referred to, respectively:

$$K^- = CT_a^2(z_0, z_1) \bar{R}(z_1, z_2) \quad (1)$$

$$K^+ = CT_a^2(z_0, z_1) \bar{R}(z_3, z_4) T_c^2 \quad (2)$$

Where, K^- and K^+ are the regressed slopes, \bar{R}^- and \bar{R}^+ are the mean aerosol scattering ratios in the regression ranges beneath and above cloud, respectively. C is lidar system constant; T_a and T_c are the transmission of aerosol and cloud, respectively. From Eq. (1) and Eq. (2), cloud optical depth can be written :

$$\tau_{cloud} = [Ln(\frac{K^-}{K^+}) - Ln(\frac{\bar{R}^-}{\bar{R}^+})] / 2 \quad (3)$$

Error sources in this method include the uncertainty of slopes from least-square regression that can be affected by non-linearity of strong signals below cloud and non-real-time molecular data, and uncertainty of mean aerosol scattering ratios. To reduce this uncertainty, we have considered special cases where cloudless data exists before the cloud observation. In this case, it is possible to estimate the mean scattering ratios above and below the cloud using the clear sky profiles obtained before the cloud.

3. AEROSOL RETRIEVALS

As an example, Fig.2 (a)~(b) show the profiles of aerosol extinction, backscatter and lidar ratio at 355-nm on March 30, 2006. To improve the raman SNR, lidar signals are averaged for 30-min duration. As we can see, the extinction and backscatter profiles are quite similar in shape thereby indicating a well-mixed boundary layer, which is also revealed by the meteorological data. Potential temperatures varied little below 2-km at both 8:00AM and 8:00PM (local time), meantime, temperature profiles showed the inversion

layer at about 2~2.5 km altitude. As shown in Fig.2 (b), mean of extinction-to-backscatter ratio of aerosol is 42.4 sr with a standard deviation 6.8 sr. This result is quite reasonable for an urban aerosol. We also note that the vertical profile of the S ratio decreases with height and is indicative of the tendency of larger particles to distribute themselves closer to the ground.

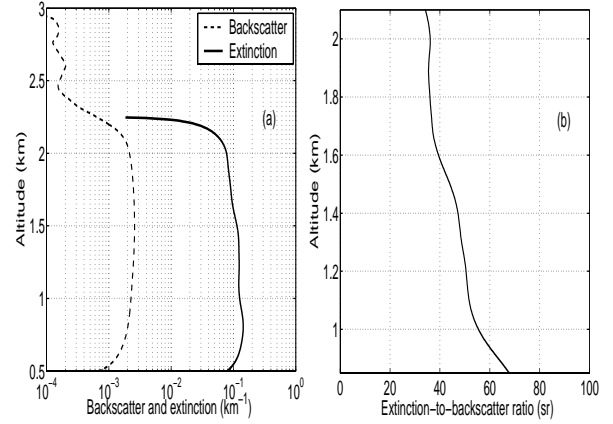


Fig.2 (a) Aerosol backscatter, extinction and (b) their ratios at 355-nm on March 30, 2006

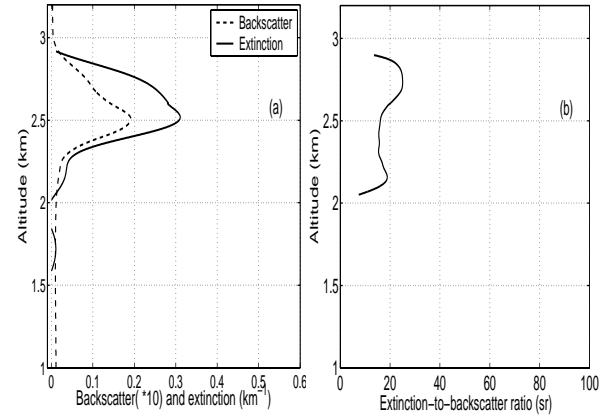


Fig3 (a) Cloud backscatter, extinction and (b) their ratios at 355-nm on March 15, 2006

4. CLOUD OPTICAL DEPTH

Low clouds are frequently measured by our Raman-Mie lidar. Fig.4 (a)~(b) show the cloud optical properties on March 15, 2006. It is clear that the cloud extends from 2~3-km altitude. Clearly, extinction-to-backscatter ratios of low cloud are much smaller than those of aerosol as indicated by Fig.2 (b) Their mean value is 18.6-sr with the standard deviation 3.9-sr. which is consistent with the previous observations and numerical analysis of water droplet clouds [5-7]. Using a

normalized gamma mode for the cloud droplet size distribution, the value of lidar ratio is calculated to be 18.9 ± 0.4 sr at 355-nm over the wide ranges of mode parameters^[6].

The time variability of cloud optical depths by both Raman- and Mie-retrievals are shown in Fig.4a. It can be seen that cloud optical depths vary from 0.3 to 0.9. The results derived by these two separate methods agree well, and furthermore, the good correlations are indicated in Fig.4b. Their correlation coefficient is as high as 0.98 with the slope of 0.88. One-to-one line is also given as reference. Slightly systematic underestimates are made by Eq. (3), especially at the large optical depths and can be partially attributed to the aerosol influences in Mie-retrieval.

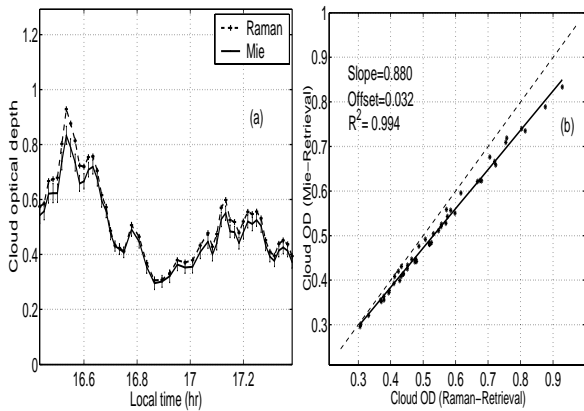


Fig.4 (a) Cloud optical depths with Raman-, elastic-returns retrieval at 355-nm and (b) their correlation on April 6, 2006

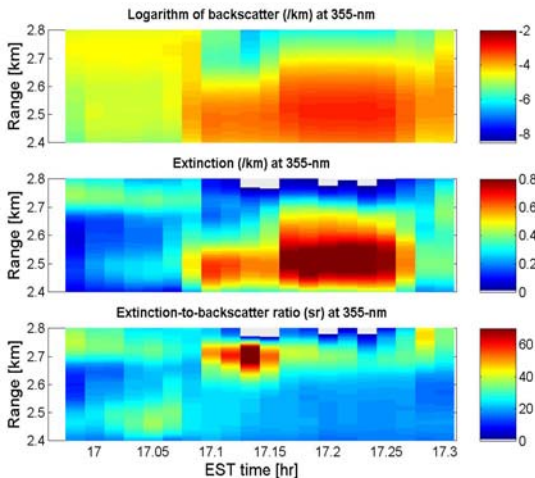


Fig 5 Extinction-Backscatter and S-Ratio in the optically thin cloud.

5. PARTICLE DROPLET SIZE

Once we have established the accuracy of the incloud extinction and backscatter profiles, we can now use these profiles to provide estimates on the size information of the water droplets. In figure 5, the combined extinction, backscatter and S-Ratio is calculated from the raman signal. The signal is averaged using a 10 minute sliding window average

To interpret this image, we again use microphysical model typical of water clouds^[6] that was Calculations using mie-scattering with the appropriate model allow us to explore the S ratio as a function of the effective particle diameter using a probe wavelength at 355 nm. The results of the mie calculation are shown in figure 6 and illustrate several important features. First, the S-ratio is fairly stable to particles from 5-30um in diameter with a value of 20. This is in agreement to the S-ratios obtained in the densest portions of the cloud which confirms the basic assumption that the cloud is primarily in the water

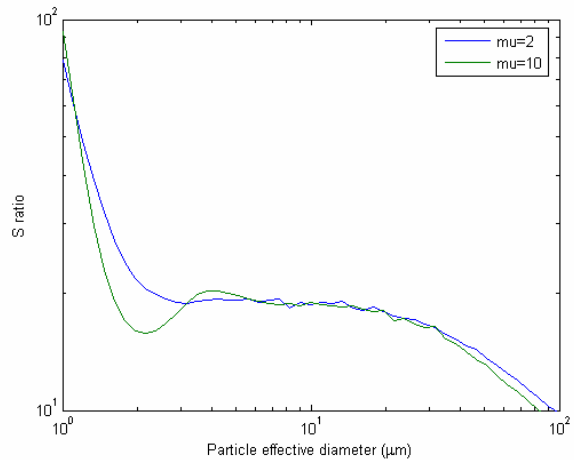


Fig 6 S ratio dependence on water droplet effective diameter based on Mie Scattering

phase. We also see that as we extend to the cloud boundaries, the S-ratio increases markedly and is indicative of smaller droplets such as would be associated either with new condensation or evaporation of the droplets near the cloud edge.

6. SUMMARY

A Mie-Raman lidar is being operated for aerosol and cloud observations in the daytime. Preliminary results are obtained concerning the extinction, backscatter and lidar ratio. In particular, optical depths of low cloud retrieved by two separate approaches show the good agreements and help validate the profiles. It was also shown that the cloud S ratio profiles could be used for preliminary sizing of effective water drop sizes and the S ratios in the clouds are consistent with water phase models. Finally, we are extending the Raman Lidar configuration to a $3\beta + 2\alpha$ configuration with the addition of a 532nm N₂ Raman channel as well as a water vapor channel. The addition of these channels will allow more accurate estimation of cloud drop diameters.

Table 1: Main specifications of Mie-Raman Lidar system at CCNY

LASER	Quanta-Ray PRO-230 Nd: YAG, 30Hz 950 mJ at 1064 nm (300 mJ at 355 nm)
Telescope	Newtonian, f/3.5, Diameter: 50.8 mm, FOV: 2mrad
Interference filters	Barr Associates Inc, Central wavelength /Bandwidth /Peak transmission Mie channel:1064,532,355 / 0.3~1 nm / T>50% N ₂ -Raman: 386.7 / 0.3 nm / T=65% 607.4 / 0.4 nm / T=60% H ₂ O(vapor)-Raman: 407.5 / 0.5 nm, / T=65% H ₂ O(liquid)-Raman: 403.2 / 6.0 nm, / T=65%
Detectors	EG&G APD Enhanced for 1064-nm Hamamatsu PMTs
Data Acquisition	LICEL TR 40-250, 12 bits and 40 MHz A/D, 250 MHz Photon-counting
Range resolution	3.75-m

ACKNOWLEDGEMENTS

This work was partially supported research grants NOAA # NA17AE1625 and NASA # NCC-1-03009.

REFERENCES

1. Ansmann A., et al., Measurement of atmospheric aerosol extinction profiles with a Raman lidar, *Opt. Lett.* 15, 746-748, 1990.
2. Whiteman D. N., et al., Raman lidar system for the measurements of water and aerosols in the earth's atmosphere, *Appl. Opt.*, 31, 3068~3082, 1992.
3. Ferrare R. A., et al., Raman lidar measurement of aerosol extinction and backscatter 1. Methods and comparisons, *J. Geophys. Res.*, 103, 19663~19672, 1998.
4. Young S. A., Analysis of lidar backscatter profiles in optical thin clouds, *Appl. Opt.*, 30, 7019~7030, 1995.
5. Ansmann A., et al., Independent measurement of extinction and backscatter profiles in cirrus clouds using a combined Raman elastic-backscatter lidar, *Appl. Opt.*, 31, 7113~7131, 1992.
6. O'Connor E.J., et al., A technique for autocalibration of cloud lidar, *J. Atmos. Ocean. Tech.*, 21(5), 777-778, 2004
7. Pinnick R.G., et al., Backscatter and extinction in water cloud, *J. Geophys. Res.*, 88(11), 6787-6796, 1983